Evaluation of a dense skin hollow fiber gas-liquid membrane contactor for high pressure removal of CO2 from syngas using Selexol as the absorbent

Bouchra Belaissaoui, Eric Favre

Evaluation of dense skin hollow fiber membrane contactor based process for CO_2 removal from high pressure syngas using Selexol as physical absorbent

Bouchra Belaissaoui *[a], Eric Favre[a]

[a] *LRGP-CNRS Université de Lorraine, 1 rue Grandville 54001 Nancy, France*

Manuscript submitted to Chemical Engineering Science

*Corresponding author: Tel: +33 372 74 37 98; fax : +33 383 32 29 75
E-mail address: bouchra.belaissaoui@univ-lorraine.fr (B.Belaissaoui)

Abstract

CO_2 removal from syngas is required for combined hydrogen production and CO_2 capture at integrated gasification combined cycle (IGCC) power plants. Conventional absorption in packed column using pressurized physical solvents such as Dimethyl Ether of Polyethylene Glycol (DEPG) (Selexol™) is largely used for this application. In this work, a dense skin hollow fiber membrane contactor (HFMC) based process for CO_2 absorption and desorption using Selexol as physical absorbent is investigated by simulation and compared to the conventional process. Thanks to the ability of dense membrane to withstand high transmembrane difference, absorbent circulates in close loop at a pressure which can be set independently of syngas pressure. Thus, contrary to the conventional process, neither absorbent depressurization before the desorber nor absorbent recompression before the absorber is needed. Under the investigated operating conditions, the process was able to recover up to 94.6 % of CO_2 with CO_2 and H_2 purity of 92.4 % and 96.6% respectively. The corresponding energy requirement for absorption and desorption loop is of 0.19 MJ_{el}/kg CO_2 which is approximately two times lower than that reported in literature under comparable gas inlet conditions and separation specifications using packed column. Without flash recovery, the corresponding H_2 loss was of 4.8%. The overall mass transfer coefficient was of $1.2.10^{-5}$ m/s and $6.8.10^{-6}$ m/s in the absorber and desorber respectively. Membrane mass transfer lower or comparable to that of absorbent combined with higher CO_2/H_2 membrane selectivity is required for H_2 loss decrease. Lower H_2 loss is achieved at the expense of increased contactor size and liquid energy pumping energy. Finally, perspectives for process optimization are exposed.

Keywords

Syngas purification, pre-combustion, physical absorbent, dense hollow fiber membrane contactor, Selexol, gas-liquid absorption

Highlights

1. Thanks to dense membrane fiber, absorbent recompression is not required for its recycling
2. Compared to packed column, the energy requirement for absorption and desorption loop can be halved
3. Without flash recovery, H_2 loss is of 4.8%
4. Process selectivity is mainly controlled by the absorbent
5. Membrane mass transfer lower or comparable to that of absorbent combined with higher CO_2/H_2 membrane selectivity is required for H_2 loss decrease.
6. Lower H_2 loss is achieved at the expense of increased contactor size and liquid energy pumping energy.

1. Introduction

Pre-combustion CO_2 capture in an integrated gasification combined cycle (IGCC) associates both CO_2 capture and H_2 production for power generation and greenhouse emission mitigation. Carbonaceous fuels are first gasified to produce the syngas which after water gas shift reaction (WGS) is composed mainly of H_2 and CO_2 (30-40% CO_2) under high pressure (20–70 bar) and temperature (190–210°C) with trace components such as H_2S, NH_3, HCN as well as heavy metals and particulates (**Scholes *et al.*, 2010)**. Acid gas (CO_2 and H_2S) removal and trace elimination are needed to fulfil the requirement for hydrogen use and CO_2 capture standards for transport and storage. In IGCC pre-combustion carbon capture (**Figure 1)**, syngas is treated to remove CO_2 prior to combustion to avoid emission of this greenhouse gas. In the purified gas, H_2 purity above 96% is generally aimed. For CO_2 capture and sequestration, CO_2 concentration should be above 90% together with low ppm level of other components (**Davidson and Metz, 2005, Padurean *et al*., 2012).**

The biggest efficiency loss associated with precombustion in IGCC is incurred in the WGS section. The latter is responsible for 44% (3.5%-points) of the total efficiency, mainly due to the use of steam for the WGS reaction. CO_2 removal section causes about 1.7%-points and the CO_2 compression and drying section are responsible for 3.0%-points efficiency loss (**Jansen *et al*., 2015**). So far CO_2 capture in IGCC power plant has only been tested and demonstrated at pilot scale (**Casero *et al*., 2014**).

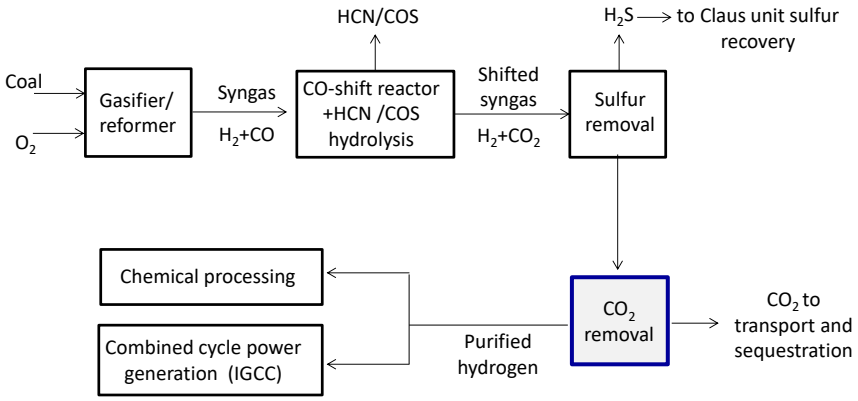

***Figure 1**: Typical IGCC and pre-combustion carbon capture process flow sheet.*

The available driving force for CO_2 capture is higher in the pre-combustion IGCC approach than in post-combustion where flue gas is typically at atmospheric pressure and contains only 4–13% CO_2. These conditions favor the use of gas-liquid absorption processes using physical solvent. Most of physical solvents are more selective for acid gas than for the main constituent of the gas (e.g. hydrogen, carbon monoxide, methane, etc.). Absorption in packed column using pressurized physical solvents such as Dimethyl Ether of Polyethylene Glycol (DEPG) (Selexol™) is largely used for acid-gas removal from high-pressure gases such as natural gas streams and syngas in a pre-combustion IGCC power plant (**Padurean *et al*., 2012, Kapetaki *et al*., 2015, Park *et al*., 2015**). Other techniques include chemical absorption, membranes and cryogenic fractionation (**Jansen *et al*., 2015**). At the difference of chemical absorbents, physical absorbents can usually be stripped of impurities by reducing the pressure without extra heating supply. The major limitations of this process are:

- In physical absorption, liquid mass transfer resistance is predominant with liquid mass transfer coefficient about two order of magnitude lower compared to chemical absorption. Moreover, non-aqueous physical solvents usually have larger viscosity compared to aqueous solvents. All this contributes to lower the mass-transfer coefficient of physical solvent which is in the range of 10^{-6}-

10^{-4} m/s while this range is of 10^{-4}-10^{-2} m/s for chemical solvents (**Chabanon *et al.*, 2014**), leading to relatively large columns size and high absorbent circulation rates.

- The need to recompress the liquid after the regeneration step: this induces a high-quality energy input (electricity), associated with a potential temperature increase of the liquid circulated in the loop. The solvent recompression step is effectively considered to require 20–30% overall energy requirement **(Gottlicher and Pruschek, 1997)**.

Thus, the possibility to either decrease the size of the installation through process intensification strategies or enable improved energy efficiency through new solvent, novel technologies, or process strategies is of great interest.

Membrane contactor is considered as one of the best promising technology to achieve intensified gas-liquid mass transfer (**Gabelman, and Hwang, 1999, Drioli *et al.*, 2005)** thanks to their very high interfacial area, up to 30 times that encountered in packed column (**Figure 2**). Given that non-aqueous physical solvents have lower surface tension compared to water and aqueous chemical solvents, they are more subject to wetting by absorbent breakthrough when porous membrane are used [**Dindore et al., 2004a**]. Thus, the use of porous membrane with physical solvents is unrealistic and the use of dense skin based HFMC is thus required. Dense membranes have indeed shown to offer a remarkable wetting protection effect because no pores are present. Moreover, in physical absorption, liquid mass transfer resistance is predominant, thus either composite or self-standing dense materials can be used. In addition, they can possibly withstand a high transmembrane pressure offering unique possibilities for increased energy efficiency as the liquid solvent can be maintained under pressure during the regeneration step.

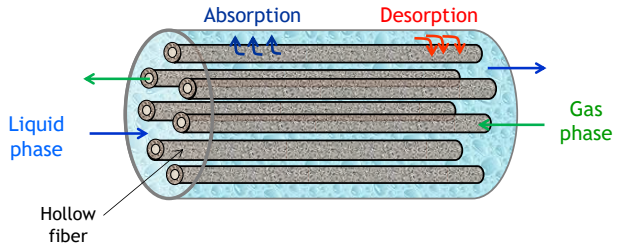

***Figure 2**: Illustration of hollow fiber membrane contactor for gas-liquid absorption and desorption*

Despite these potentialities, a limited number of studied investigated however the technology with non-aqueous physical solvents for this application **(Chabanon *et al.*, 2014)**. The potentiality of either composite or self-standing dense materials remains largely unexplored for CO_2 removal from high pressure syngas streams using physical absorbents. Additionally, to our knowledge, the evaluation of process intensification and energy requirement of HFMC for this application, using the potentialities exposed above and offered by dense membrane contactor has not been addressed.

This paper focus on the evaluation of intensification and energy penalty reduction of CO_2 removal section using membrane contactor technology compared to absorption in packed column technology using (DEPG) (Selexol™) as physical solvents. The evaluation of dense skin HFMC based process for CO_2 absorption and desorption for the treatment of high pressure acid gas streams using physical absorbents is proposed. The concept is illustrated in the case of shifted syngas treatment using Selexol as absorbent and the performance is compared to the reference packed column technology.

First, a brief presentation of conventional packed column for acid gas removal by physical solvent is given. Second, the novel process based on dense skin HFMC is shown and its potentialities highlighted. Then, a state of the art of dense skin membrane HFMC for CO_2 removal using physical solvents is

presented. Next, modeling and simulation framework is presented. Finally, the simulation results are shown and the performance of HFMC based process is compared to state of the art packed column for CO_2 removal from shifted syngas.

2. Conventional packed column for acid gas removal by physical solvent

Depending on the degree of contaminant removal and their concentration in the feed gas, a wide variety of regeneration schemes are available (**Kohl and Nielsen, 1997).**

The simplest version of a physical solvent process involves absorption followed by regeneration of the solvent by flashing to atmospheric pressure or vacuum, or by inert gas stripping (**Figure 3**)(**Kwak *et al*., 2014).** In order to limit valuable product loss, the solvent leaving the absorption column is transferred to a flash tank where dissolved non-acidic gases are released and returned back to the absorber. If important H_2S amount is present, then H_2S removal, typically achieved by using Selexol as absorbent, prior to CO_2 removal is required. One of the most important process factor impacting energy and capital cost is the solvent circulation rate. The latter can be reduced by decreasing temperature, thus increasing the acid gas absorption solvent capacity. Another benefit from cooling the solvent is the reduction of the absorbed amount of H_2 present in the shifted syngas application as the latter solubility shows generally little change with temperature **(Kapetaki et al., 2015)**. However, decreasing solvent temperature increases its viscosity thus resulting in reduced solvent mass transfer performances and increased solvent pressure drop.

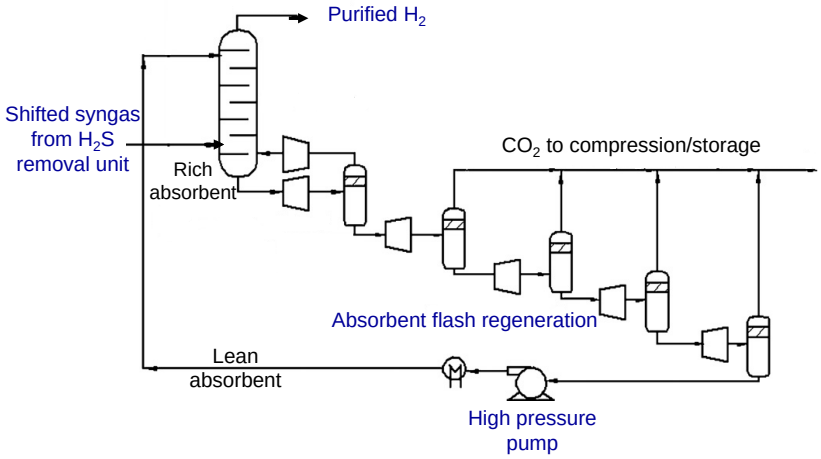

***Figure 3**: Process flow diagram of a typical physical solvent process for absorption of acid gases from feed gas streams.*

A number of physical solvents are available for use in acid gas treating processes (**Kohl and Nielsen, 1997)**. Typical operating conditions of commercial physical solvent processes and main characteristics are given in **Table 1.** Data of gas solubility and industrial physical absorbents selectivities as well as their main physico-chemical properties is given in **Appendix A,** in **Table A1** and **Table A2** respectively.

***Table 1**: Operating conditions of commercial physical solvent processes and main characteristics.*

Process	solvent	Absorption conditions	Main characteristics
Selexol	Dimethyl Ether of Polyethylene Glycol (DEPG)	-10°C to 40°C, 20 to 50 bar [a,b,d,e]	Efficient for both CO_2 and H_2S removal High selectivity for H_2S over CO_2 Higher viscosity
Rectisol	Methanol	-40 to -60°C[abc], 20 to 36 bar [d,a]	Good H_2S and CO_2 removal efficiency High purity cleaned gas Requires more electrical energy for refrigeration
Purisol	NMP (N-Methyl-2-Pyrrolidone)	-20 to 40[d], 40 to 70 bar [d,a]	High selectivity for H_2S over CO_2 More volatile solvent Need water washing
Morphysorb	Morpholine	49°C, 69 bar [a]	Selective removal of H_2S and CO_2 High solvent capacity load Low process maturity level
Fluor	Propylene carbonate	-17 to 25 °C [a], 30-70 bar [d,a]	High solubility of CO_2 Uneconomical to achieve high product purity

[a] Theo *et al.*, 2016 , [b] Padurean *et al.*, 2012, [c] Jansen *et al.*, 2015 , [d] *Kohl and Nielsen*,1997, [e] Park *et al.*, 2015.

3. Novel process based on dense HFMC for CO_2 absorption and desorption using physical absorbents

The principle of the use of dense skin based membrane for the absorption and desorption under high pressure is shown in **Figure 4**. **Figure 5** shows the novel dense skin HFMC based absorption/desorption loop for CO_2 removal from shifted syngas. First, the shifted syngas enters the absorber under high pressure (20 to 70 bar). The gas leaving the absorber has an increased concentration of H_2. CO_2 removal above 90% is typically aimed. The CO_2 enriched absorbent with some dissolved H_2 leaving the absorber is sent to the desorber, without its depressurization. Indeed, as explained above, dense membrane is able to withstand high transmembrane pressure difference. CO_2 is stripped from the rich solvent using vacuum pumping or sweep gas. The regenerated absorbent leaving the desorber is recycled back to the absorber in a closed loop.

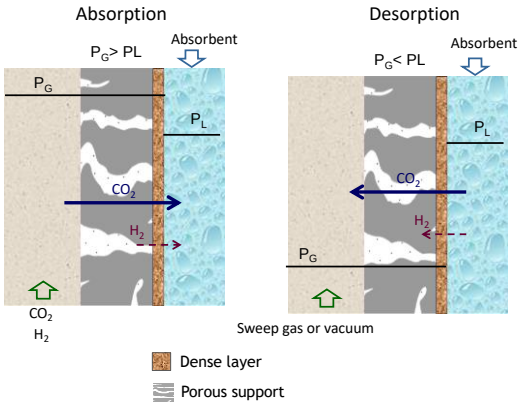

***Figure 4:** Illustration of absorption and desorption using dense skin based membrane contactors. CO_2 removal from shifted syngas.*

The main advantages of this novel approach are the following:

(i) Thanks to the ability of dense membrane to withstand high transmembrane difference, absorbent circulates in close loop at a pressure which can be set independently of syngas pressure. Thus, neither absorbent depressurization before the desorber nor absorbent recompression before the absorber is needed.

(ii) Liquid recompression is not required before it is recycled to the absorption step. Thus, compared to the conventional process, the high pressure pump, the flash vessel and the heat exchanger are substituted by a simple pump leading to a significant decrease of the energy requirement of the process (i.e. OPEX). A single cheap equipment (circulating pump) is needed, which generates lower capital expenses (i.e. CAPEX).

(iii) CO_2/H_2 selectivity of dense skin is typically up to 5 for polymeric membranes, up to 12 for advanced cross-linked membrane and up to 100 for advanced facilated transport membranes (**Scholes et al., 2012)**. This offers possible H_2 loss limitations.

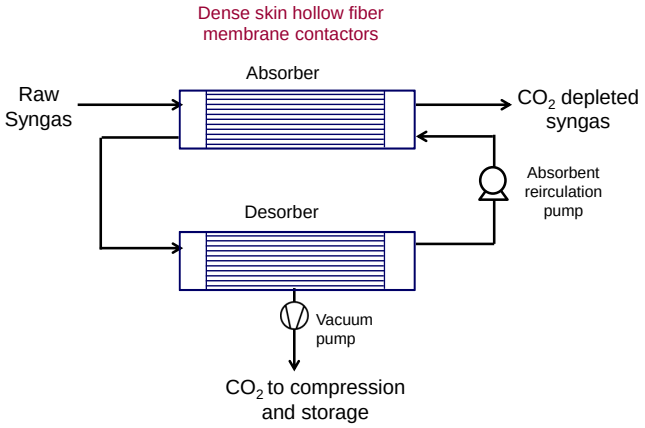

Figure 5: *Scheme of the proposed process based on dense HFMC for CO_2 absorption and desorption using physical absorbents*

4. Dense membrane based HFMC for CO_2 absorption/desorption using physical solvent : a state of the art

Experimental studies investigating physical absorbent for CO_2 absorption or stripping using dense skin based membrane contactor are summarized in **Table 2. Trusov *et al*., 2011** studied high permeability glassy polymers such as PTMSP, PTMGP and PMP for acid gas removal processes at conditions which are typical for the regeneration of physical solvents (water, propylene carbonate, N-Methyl-2-pyrrolidone-NMP) and chemical solvents (MEA, MDEA, PZ). They presented a detailed chemical, physical stability of glassy membranes in contact of aforementioned solvents at 100°C during 300 h (membrane samples was soaked in the absorbent). No detectable chemical changes in the polymer structure or macroscopic properties were evidenced. They showed experimentally that water and alkanolamines can be regenerated by pressure and temperature swing (Δp_m = 40 bar, T = 100 °C) in the investigated gas–liquid contactors. In **Dai *et al.,* 2016b,** membrane contactors using nonporous polymeric hollow fiber membranes with ionic liquids as absorbent were tested experimentally for pre-combustion CO_2 capture at elevated temperature and pressures (80°C, 1 to 20 bar). A CO_2 flux of about 2×10^{-4} mol.m^{-2}.s^{-1} was obtained using nonporous Teflon-PP membrane contactor at 10 bar with a gas flow rate of 100 ml.min^{-1} and liquid flow rate of 20 ml.min^{-1}. The Teflon-PP composite membrane exhibited good stability in a 14 days test.

To our knowledge, no studies reported on long term stability during absorption or desorption experiments of non-aqueous physical absorbent under high temperature and transmembrane pressure. In all the reported studies using physical solvent and membrane contactor presented briefly above, no values have been given of energy requirement and overall CO_2 flux under relevant industrial conditions and product specification of gas absorption and desoption, and compared to the reference packed column technology.

Regarding the mechanical resistance of dense membranes, **Trusov et al., 2011** showed experimentally that symmetric glassy membrane (thickness of 20μm to 40μm) can operate successfully under transmembrane pressure difference of 40 bar when tested for CO_2 desorption from pressurized water. Based on theoretical calculation, it has been shown that a thickness as low as 5μm can support up to 10 bar transmembrane difference (**Chabanon *et al*., 2014**).

Dense skin thickness varies typically between 2 to 10 μm for PDMS (polydemythyl siloxane) and 0.1 to 1 μm for PMP (polymethylpentene) (**Nguyen *et al*., 2011, Falk-Pedersen and Dannstroem)**. Dense skin membranes based on polydemythyl siloxane (PDMS), poly[1-(trimethylsilyl)-1-propyne] (*PTMSP*) and Teflon AF2400 on microporous PP supports are among the more CO_2 permeable membranes. Commercial selfstanding dense membranes based on PDMS or Teflon AF 2400 shows $k_{m,CO2}$ around 10^{-5}m/s with membrane thickness of 30 to 200 μm (**Ozturk and Hughes, 2012, Heile *et al*., 2014)**. CO_2 membrane mass transfer coefficient of composite or self-standing dense materials can range between 10^{-3} to 10^{-5} m/s depending on the membrane material and dense skin thickness.

Among commercially available polymeric membranes, rubbery polymers such PDMS and Pebax 3533 are considered as good candidates for CO_2/H_2 separation thank to their high permeances, albeit their low selectivity. Their performance is limited by the Robeson upper bound for CO_2/H_2 separation as shown in **Figure B1 in Appendix B.**

Table 2: *Non-porous membranes for CO_2 absorption and stripping using non-aqueous physical absorbent*

References	Feed gas	T	Pressure conditions	Absorbent	membrane	comments
Dai *et al.,* 2016 *CO_2 Absoption*	CO_2 45%/He 55%	80°C	P_G=1-20bar $P_G/P_L \approx 1$	Ionic liquid : [Bmim][TCM][1]	Composite Teflon-Polypropylene (PP), porous PTFE	Better stability compared to porous PTFE[2] membranes in 14 days test, at 20 bar and 100°C.
Trusov *et al.,* 2011 *Chemical and physical Stability tests*	Pure CO_2	100°C	-	Water, propylene carbonate, NPM[3]	Symmetric glassy membranes : PTMS[4], PMP[5], PTMGP[6]	No changes in the chemical structure and macroscopic properties of those polymers, on long term tests under at 100°C during 300 h
Chabanon et al., 2014 *CO_2 desorption*	N_2 as a sweeping gas	Amb.	P_G= 1 atm P_L=2 bar	Selexol	Dense self-standing PDMS[7]	Unsteady state selexol-CO_2 saturated regeneration was operated successfully. No long term tests.

[1][Bmim][TCM]: 1-Butyl-3-methylimidazolium tricyanomethanide PTMSP: poly[1-(trimethylsylil)-1-propyne], [2]PTFE : Polytetrafluoroethylene, [3]NMP: *N*-Methyl-2-pyrrolidone, [4]PTMSP : poly[1-(trimethylsilyl)-1-propyne], [5]PMP: poly[4-methyl-2-pentyne] ,[6] PTMGP : poly[1-(trimethylgermil)-1-propyne], [7]PDMS: polydemythyl siloxane.

High performing membranes include mixed matrix membrane (MMMs), facilated transport fixed site

carrier membranes (FSCM), thermally rearranged polymers, and polymers with intrinsic micro-porosity (PIMS). Examples of polymeric membrane for CO_2/H_2 separation are shown in **Table B2**.

5. Simulation framework

5.1. 1D model – resistances in series model description

The membrane module has been modelled according to a 1D resistances in series approach, similarly to previous studies dedicated to gas-liquid absorption processes using HFMC **(Cui and Demontigny, 2013, Albarracin Zaidiza *et al*., 2014, 2016, 2016, Kerber *et al*., 2016)**. The simulation methodology of the HFMC based absorption/desorption process is shown in **Figure 6.** A 1D modeling strategy systematically separately considers the three different mass transfer domains shown in **Figure 7** in order to determine the effective local mass transfer coefficient of each species..

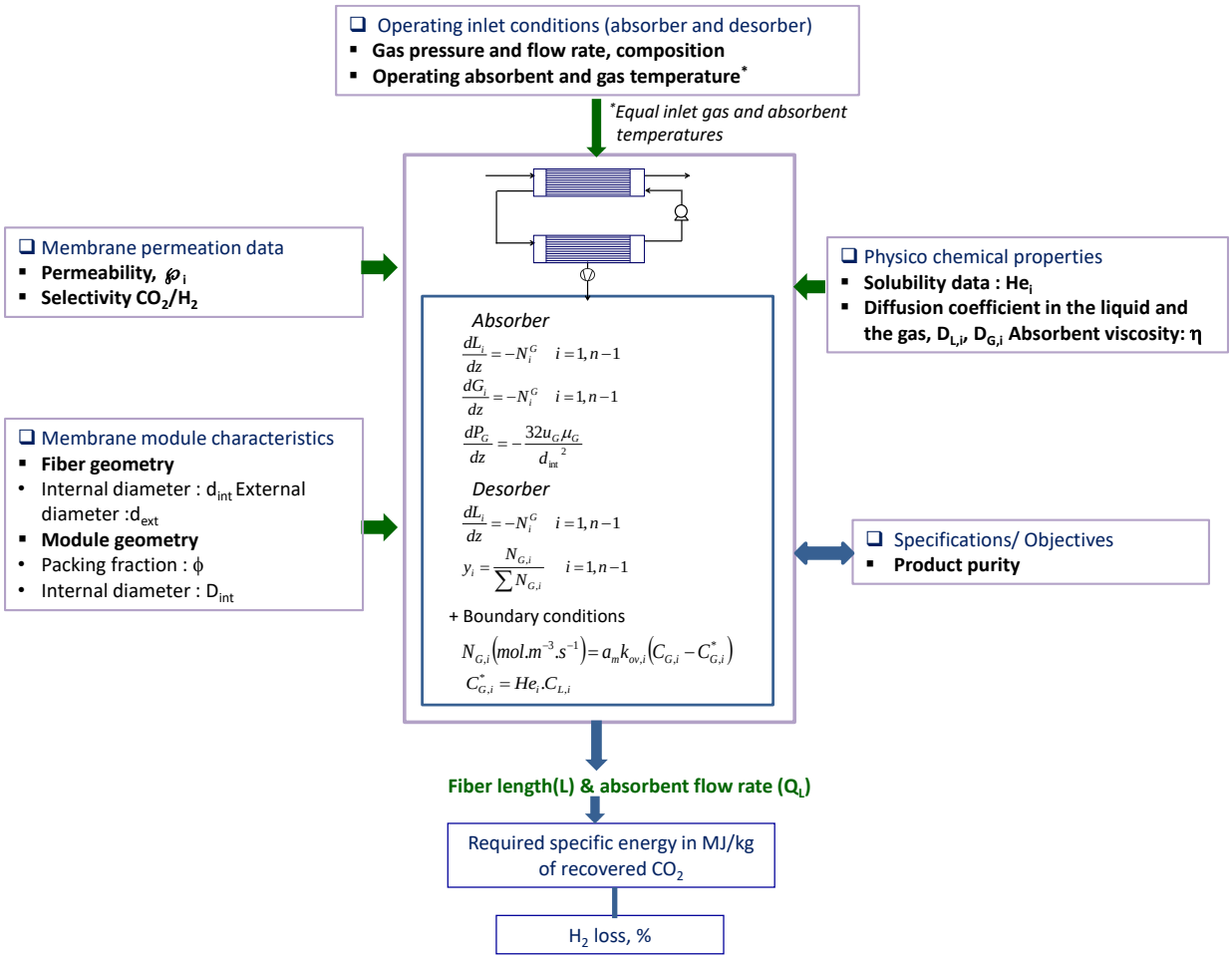

Figure 6 : *Scheme of the simulation methodology*

For all simulations, the liquid circulates in the shell side of the fiber while the gas flows in the lumen side. The 1D model takes into account the evolution of the local mass transfer coefficients, the evolution of gas velocity (due to CO_2 absorption) and fluid pressure through the axial coordinate (z). In the absorber, the flow is counter-current with plug flow assumed in both gas and liquid phases. In the

desorber, cross plug flow is considered with plug flow assumed for the liquid phase and free flow (perfect mixing) in the gas phase. Moreover, absorption and desorption processes are assumed to be isothermal. In **Appendix C**, details on model assumptions, gas and liquid mass transfer coefficient calculation as well as the equation system solved using Matlab software are presented.

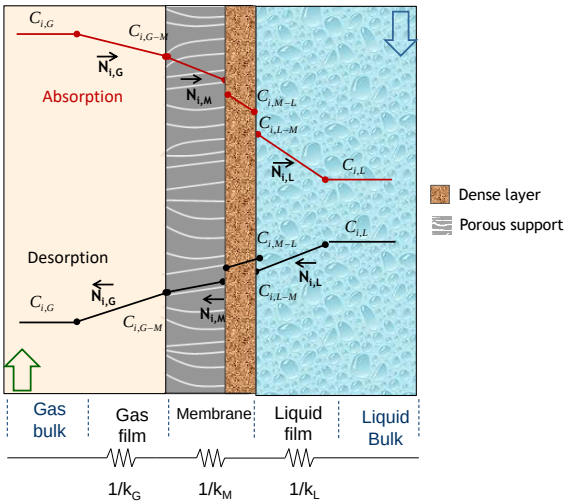

Figure 7: *A schematic representation of the resistance in series based on film theory*

5.2. Characteristics of the HFMC module

Geometrical characteristics of the hollow fiber membrane module (HFMC) are illustrated in **Figure 8**. In the simulation, the fiber geometry of commercial PPO (Parker P-240) is considered. The packing density and the module internal diameter were set at 0.5 and 36 cm respectively, which is typical of industrial modules. The characteristics of the membrane module are summarized in **Table 3**.

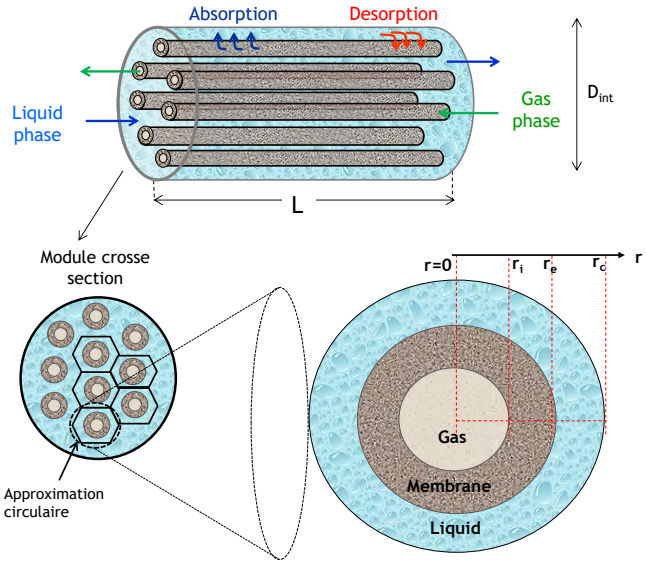

Figure 8: Geometrical characteristics of the hollow fiber membrane module (HFMC)

***Table 3**: Characteristics of the membrane module for all simulations.*

	Characteristics	Value
Module	Inner diameter (m), D_{int}	0.36
	Packing ratio (-), ϕ	0.50
	Fiber number (-), N	$2.39.10^5$
	Mean log specific interfacial area (m^{-1}), a	3260
Fiber	Inner diameter(μm), d_{int}	370
	Outer diameter(μm), d_{ext}	520

5.3. Physico-chemical data and operating conditions

In the simulation the gas is considered to be a binary CO_2/H_2 mixture, composed of 40% CO_2 and 60% H_2 (typical composition of a shifted syngas). Water is supposed to be available at 15°C. The gas feed is considered to be at 36 bar and 35°C [**Kapetaki *et al*., 2015, Padurean *et al*., 2012, Dave *et al*., 2016**] according to typical relevant industrial conditions for syngas separation. The vacuum pressure for CO_2 stripping was set at 300 mbar.

The operating conditions considered in the simulations are summarized in **Table 4**. The simulation is achieved considering typical available polymeric membrane such as PDMS based membranes with $k_{M,CO2}=5.10^{-4}$ m/s and CO_2/H_2 selectivity of 4*,* for both absorber and desorber. The physico-chemical properties and phase equilibria of the system at 35°C are shown in **Table 5**.

Table 4: Operating conditions of all simulations

	Absorber	Desorber
Gas inlet composition	62% H_2 , 38% CO_2	Vacuum pumping
Temperature (°C)	35	35
Gas inlet flowrate (Nm^3/h)	116.9	-
Gas inlet pressure (bar)	36	0.3
Gas interstitial velocity (m/s)	0.04	-

***Table 5** : Physico-chemical properties and phase equilibria data of the system at 35 °C*

	CO_2	H_2
Henry's constant (-) $(C_G/C_L)eq$ [a]	0.404	25.79
Diffusion coefficient in liquid phase (m^2/s) [b]	$2.6.10^{-10}$	$3.6.10^{-10}$
Diffusion coefficient in gas phase (m^2/s) [c]	$1.38.10^{-5}$	$6.35.10^{-5}$
Absorbent solubility selectivity CO_2/H_2 (-)	63.83	
Absorbent viscocity (10^{-3} Pa.s) [b]	4.37	

[a] Kapeteki et la., 2015, [b] Heintz, 2011 , [c] Chapman and Enskog theory

5.4. Process performances and energy requirement

The main performance indicators to be evaluated for gas-liquid HFMC for CO_2 removal from syngas are:

- The average overall CO_2 mass transfer coefficient $k_{ov,CO2}$ in m/s
- The product of $k_{ov,\,CO2}$×a in s^{-1}, with a the specific membrane surface area in m^{-1}
- Average CO_2 specific absorbed flux in $mol/m^3.s$
- CO_2 removal efficiency,η CO_2 (-)

- Process specific energy requirement in MJ/Kg of recovered CO_2

By writing a mass balance across a differential section of the membrane contactor, then integrating over the length of the contactor, the average overall CO_2 absorbed flux and overall mass transfer coefficient K_{ov} is calculated.

The CO_2 removal efficiency η_{CO2} can be calculated as:

$$\eta_{CO2} = \frac{G_{abs,in} \times y_{CO2,in} - G_{abs,out} \times y_{CO2,out}}{G_{abs,in} \times y_{CO2,in}} \quad (1)$$

With y, mole fraction in the gas phase and G, molar gas flow rate.

For the HFMC process, the energy requirement for the HFMC based depicted in **Figure 5** is the summation of diferent contributions:

- Absorbent pumping power requirement for the recirculation of absorbent (selexol) in closed loop, $P_{L,p}$
- Power required for vacuum pumping in the desorber to strip CO_2 from CO_2-loaded absorbent, P_{vacuum}

The required energy demand for absorbent pumping is calcuted fom the solvent flow rate, Q_L, and total liquid pressure drop ΔP_L by :

$$P_{L,p} = \frac{1}{\eta_p} Q_L . \Delta P_L \quad (2)$$

η_p is the pump efficiency, set to 0.6.

To estimate the power requirement of the vacuum pump for absorbent regeneration, isentropic compression was assumed:

$$P_{vacuum} = \frac{1}{\eta_V} G_{des} \frac{\gamma RT}{\gamma - 1} \left[\left(\frac{P_{atm}}{P_{G,des}} \right)^{\frac{\gamma-1}{\gamma}} - 1 \right] \quad (3)$$

G_{des} and $P_{G,des}$ are the molar flow rate and pressure of the stripped gas in the desorber, respectively. η_V, set to 0.74, is the vacuum pump efficiency. γ is the adiabatic expansion factor of the gas mixture.

6. Results and discussion

Figure 9 shows the simulation results of the investigated process. Streams flow rates and concentrations are also indicated. **Figures 10a and 10b** show the axial profile of CO_2 and H_2 transmembrane flux in the absorber and desorber respectively. H_2 flux increases from the gas inlet as the driving force between the two phases increases. An inverse profile is observed for CO_2. CO_2 flux is minimal at the gas outlet where CO_2 content is low (near 3%) and where the driving force between the two phases is minimal. In the desorber CO_2 and H_2 follow the same trend as the CO_2 in the absorber. Fluxes are maximal at the liquid inlet (CO_2 and H_2 loaded solvent) and decreases as the gaseous species are desorbed from the liquid phase.

The energy requirement, overall mass transfer coefficient of both absorber and desorber are shown in **Table 6**. The proposed dense HFMC was able to recover up to 94% of CO_2 with 92.4% purity. The recovered H_2 purity is of 96.6%. The corresponding energy requirement is of 0.19 MJ_{el}/kg CO_2, which is approximately over 2 times lower than that reported under comparable gas inlet conditions and separation specifications as can be seen in **Table 8**.

However, the obtained H_2 loss is of 4.8% which is significantly higher than that reported for conventional packed column based process (less than 1%) (**Park et al., 2015)**. In the latter, first flash

thank is used to recover H_2 from rich absorbent. The recovered H_2 is then recycled to the inlet of the absorber (**Figure 2**). In order to limit H_2 loss using the concept of membrane contactor proposed in this work, a configuration using a flash at medium pressure to recover a portion of H_2 before entering the desorber contactor need to be investigated.

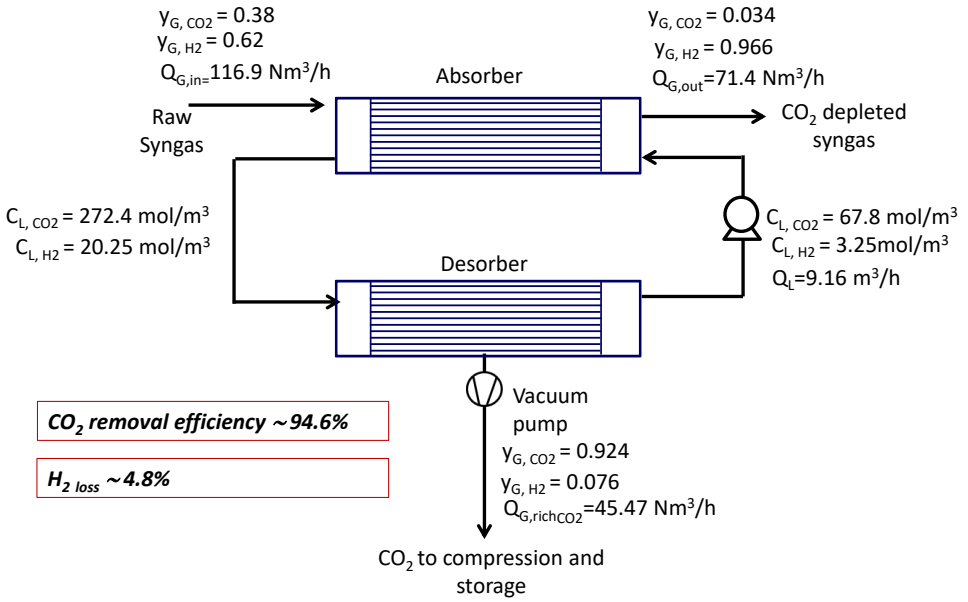

Figure 9: *Simulation results of the HFMC process for CO_2 removal from syngas using Selexol as physical absorbent. Partial regeneration of the absorbent. $k_{M,CO2}$=5.10^{-4} m/s, CO_2/H_2 selectivity of 4.*

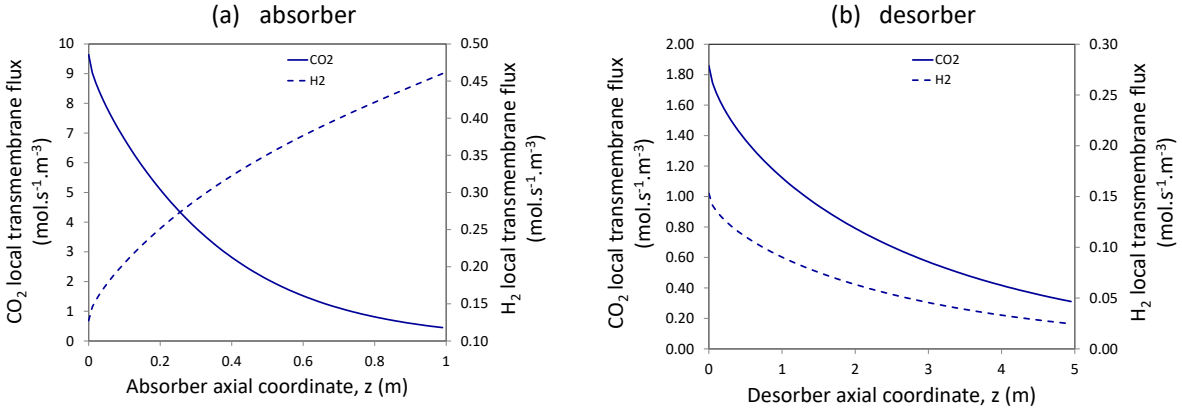

Figure 10: CO_2 and H_2 transmembrane flux profiles along the absorber. (a) absorber (b) desorber. z=0 corresponds to the gas inlet.

The $k_{ov, CO2}.a$ values obtained in this work are of 0.04 and 0.02 s^{-1} for the absorber and the desorber respectively. The average CO_2 specific absorbed flux is of 5 mol/m^3.s. These values can be used for comparison to packed Column technology under the same operating conditions allowing volume reduction potential calculations.

Table 6: Summary of simulation results

Absorber liquid pressure drop (bar)	0.63
Desorber liquid pressure drop (bar)	3.15
Absorber length	1
Desorber length	5
Liquid flow rate (m^3/h)	9.16
Interstitial liquid velocity (m/s)	0.05
Liquid recirculation (pumping) (MJ/kg recovered CO_2)	0.0709
Vacuum pump regeneration (MJ/kg recovered CO_2)	0.119
Total specific energy requirement (MJ/kg recovered CO_2)	0.19
k_{ov} ($m.s^{-1}$) abs/des	$1.2.10^{-5}$ /$6.8.10^{-6}$
k_{ov}. a (s^{-1}) abs/des	0.0388/0.022
Average CO_2 specific absorbed flux ($mol/m^3.s$)	5.10
Average CO_2 specific stripped flux ($mol/m^3.s$)	1.02
CO_2 recovery ratio (%)	94.6
H_2 purity (%)	96.65
H_2 loss %	4.8%

Process selectivity analysis

Applying the resistance in series based on film theory (Equation 10) and considering flat membrane with neglecting gas side mass transfer resistance, overall mass-transfer coefficient of specie *i* can be expressed as follows:

$$\frac{1}{k_{ov,i}} = \frac{1}{k_{m,i}} + \frac{He_i}{k_{L,i}} \qquad (4)$$

Overall process selectivity can be determined as the ratio of the overall mass transfer coefficient of the species to be separated *i* and *j (*Kerber et al., 2016):

$$S_{ov,ij} = \frac{k_{ov,i}}{k_{ov,j}} = \left(\frac{1}{k_{m,j}} + \frac{He_j}{k_{L,j}}\right) \Big/ \left(\frac{1}{k_{m,i}} + \frac{He_i}{k_{L,i}}\right) \qquad (5)$$

The selectivity of the solvent, $S_{Abs,\ i/j}$ is mainly given by the ratio of gaseous species solubility in the absorbent as liquid mass transfer coefficient of species *I* and *j* does not differ significantly in physical absorbent [**Kerber et al., 2016**]:

$$S_{Abs,ij} = \frac{He_j}{He_i} \qquad (6)$$

The selectivity of the membrane, $S_{M,\ i/j}$ is defined as the ratio of membrane mass transfer coefficient of species *i* and *j*:

$$S_{M,ij} = \frac{k_{M,i}}{k_{M,j}} \qquad (7)$$

Membrane selectivity is also referred to as ideal selectivity α defined as a ratio of species permeabilities or permeance $J_{M,i}$ in mol/(m^2.s.pas):

$$\alpha_{ij} = \frac{\wp_i}{\wp_j} \qquad (8)\ \text{With:}$$

$$k_{M,i} = J_{M,i} RT = \frac{\wp_i}{e} RT \qquad (9)$$

With *e* is the dense skin thickness of the membrane.

Integrating the two last equations in Equation 3 gives:

$$S_{ov,ij} = \frac{\alpha_{ij} + He_i \times S_{Abs} / (k_L / k_{M,i})}{1 + He_i / (k_L / k_{M,i})} \qquad (10)$$

The overall selectivity of the process is expressed as a function of both the selectivity of the membrane and that of the liquid as well as solubility of specie *i* and the ratio $k_L / k_{M,i}$.

Considering laminar regime and developed concentration profile (Gr>0.03), Sherwood number is constant and so is k_L for a given hydraulic diameter (Equation 1 and 2). Considering typical hydraulic diameter of 520 µm used in this study, the K_L value for CO_2 at 35°C in Selexol is of $2.2.10^{-6}$ m/s.

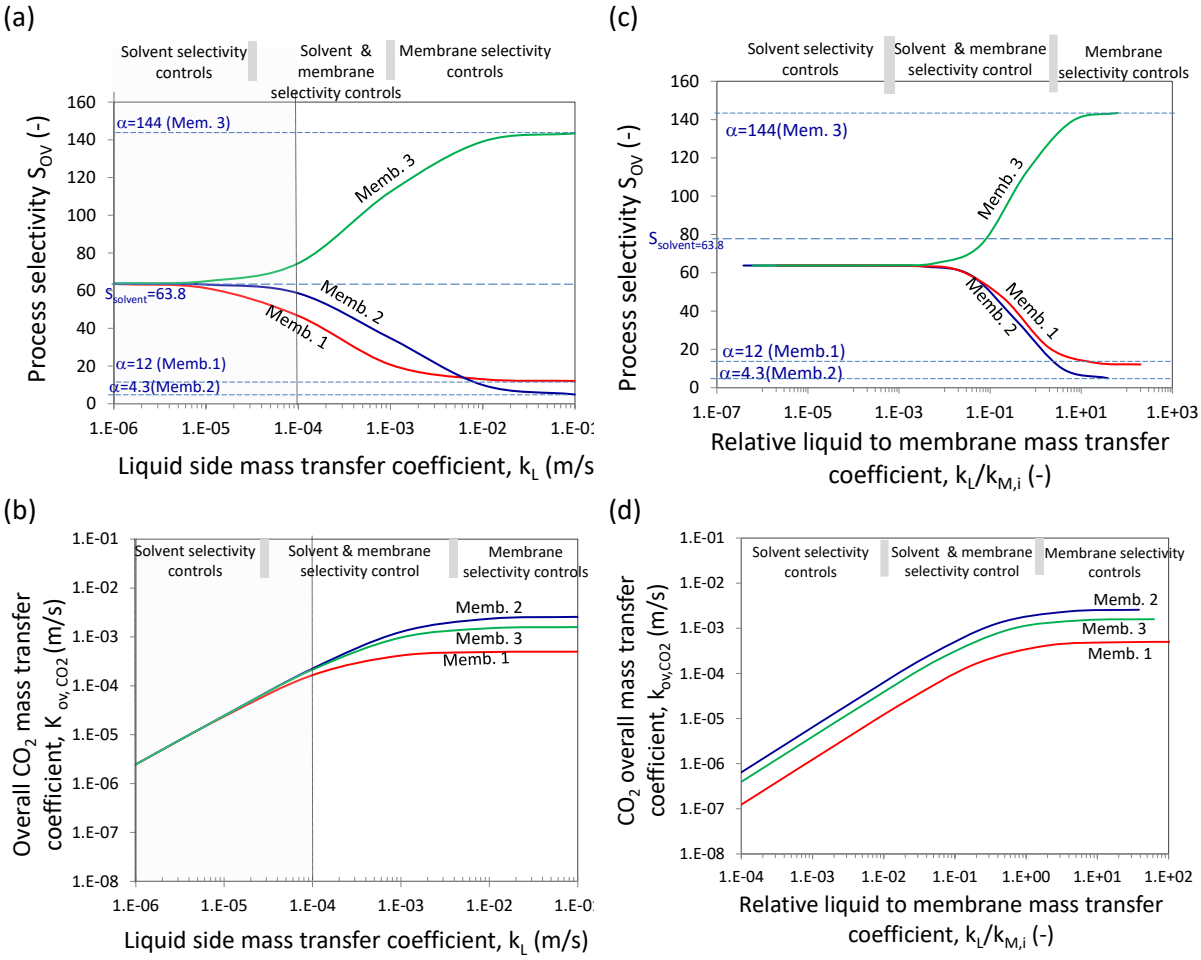

Figure 11: Process selectivity (a) and overall CO_2 mass transfer coefficient (b) as function of liquid mass transfer coefficient. Figures (c) and (d), represent the same plots than (a) and (b) with the abscess corresponding to relative liquid to membrane mass transfer coefficient. Memb.1: $k_{m,CO2}$= 5.10^{-4}m/s, $\alpha_{CO2/H2}$= 12. Memb.2: $k_{m,CO2}$=$2.6.10^{-3}$ m/s, $\alpha_{CO2/H2}$= 4.3. Memb.3: $k_{m,CO2}$=$1.6.10^{-3}$ m/s, $\alpha_{CO2/H2}$= 144. Selexol as absorbent, T=35°C. $K_{L,\,CO2}$= $2.2.10^{-6}$ m/s.

Figure 11 shows process selectivity and overall CO_2 mass transfer coefficient as function of liquid mass transfer coefficient and relative liquid to membrane mass transfer coefficients. Results are shown for three membranes noted Mem1, Mem2 and Mem3 (see Table B2).

When reporting, in **Figure 11a, the** k_l value for CO_2 at 35°C in Selexol is of $2.2.10^{-6}$ m/s, it can be seen that process selectivity is mainly controlled by the selectivity of the solvent. However as liquid to membrane mass transfer increases (i.e. decreased membrane mass transfer), membrane selectivity starts to control progressively the overall process selectivity. Thus, theoretically, membrane mass transfer lower or at most comparable to that of absorbent mass transfer coefficient combined with higher CO_2/H_2 selectivity than that of the absorbent is required to increase the CO_2/H_2 process selectivity.

According to this discussion, we have achieved simulations considering membrane CO_2 mass transfer coefficient of 2.10^{-6} m/s while keeping constant all other operating conditions at the same value than in the first set of simulations (temperature, pressure, inlet gas concentration, fluid flow rates). The results are shown in **Figure 12**. The energy requirement, overall mass transfer coefficient of both absorber and desorber are shown in **Table 7**. The proposed dense HFMC was able to recover up to 93.8% of CO_2 with 93.8% purity. The recovered H_2 purity is of 96.3%. Interestingly, H_2 loss is reduced to 1.3%. In order to attain these performances, membrane CO_2/H_2 selectivity of 300 was required. Such high selectivity has been reported experimentally for facilated transport membranes (See Table B1). Indeed, facilated transport fixed site carrier membranes (FSCM) have been reported to show high CO_2 permeability and selectivity for low CO_2 pressures prevailing in post-combustion capture applications. However, their ability to perform under high pressure pre-combustion capture application is very questionable due to carrier saturation under high CO_2 partial pressure [**Rafiq et al., 2016**]. High performances for this type of membranes have not been evidenced under relevant industrial conditions in pre-combustion application.
Compared to the first set of simulations, the required absorber and desorber length increased about 5 times. The corresponding energy requirement is of 0.446 $MJ_{el}/kg\ CO_2$, which is approximately over 2.3 times higher than that in the first set of simulations. Moreover, it can be seen that achieving lower H_2 loss is at the expense of increased contactor size and liquid energy pumping energy.
A systematic and detailed parametric analysis is of interest in order to evaluate the HFMC absorption/desorption loop process for a wide range of operating conditions and achieve parametric and process design optimizations. This important work will be presented in a forthcoming paper.

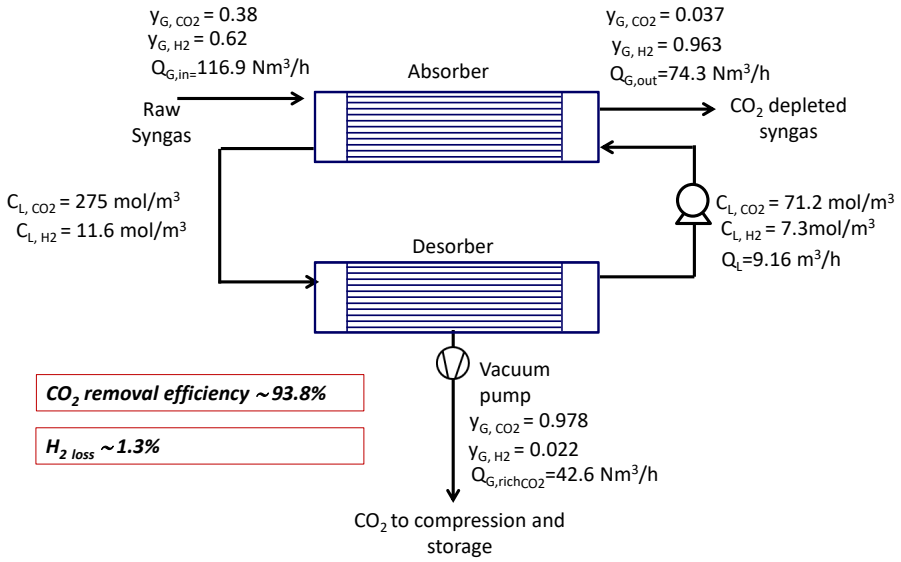

Figure 12: *Simulation results of the HFMC process for CO_2 removal from syngas using Selexol as physical absorbent. Partial regeneration of the absorbent. $k_{M,CO2}$=2.10^{-6} m/s, CO_2/H_2 selectivity of 300.*

Table 7: Table 12: Simulation results of configuration 2, membrane A in the absorber. Hypothetic membrane in the desorber: $k_{m,CO2}$ value of 1.10^{-6} m/s, membrane CO_2/H_2 selectivity : 520.

Absorber liquid pressure drop(bar)	3.78
Desorber liquid pressure drop (bar)	13.86
Absorber length	6
Desorber length	22
Liquid flow rate (m³/h)	9.16
Interstitial liquid velocity (m/s)	0.05
Liquid recirculation (pumping) (MJ/kg recovered CO_2)	0.334
Vacuum pump regeneration (MJ/kg recovered CO_2)	0.112
Total specific energy requirement (MJ/kg recovered CO_2)	0.446
k_{ov} (m.s^{-1}) abs/des	1.9.10^{-6} /1.5.10^{-6}
k_{ov}. a (s^{-1}) abs/des	0.006/0.005
Average CO_2 specific absorbed flux (mol/m³.s)	0.84
Average CO_2 specific stripped flux (mol/m³.s)	0.23
CO_2 recovery ratio (%)	93.8
H_2 purity (%)	96.32

Table 8: Comparison with literature data

Solvent/process	CO_2 and H_2 Feed gas content	H_2 loss %	Operating conditions	CO_2 capture %	Total specific power consumption MJ_{el}/kg_{CO2}
This study (simulation 1)	38% CO_2 62% H_2	4.8	T =35°C P =36 bar	94.5	0.19
This study (simulation 2)	38% CO_2 62% H_2	1.3	T =35°C P =36 bar	93.8	0.446
Kapetaki *et al*., 2015	37.76% CO_2 56.33% H_2	1%	T =35°C P =36 bar	90	0.4638
Mohammed *et al*., 2014	-	-	-	90-91	0.389 (0.1080 kwh/kg CO_2)

7. Conclusions and perspectives

This study intended to evaluate the potentialities of dense skin membrane contactors for shifted syngas purification using Selexol as physical absorbent considering absorption/ desorption loop. This topic has been indeed surprisingly unexplored, compared to CO_2 absorption into chemical solvents.
Through simulations, the following conclusions have been obtained:

(i) Using commercially available membrane performance, the novel HFMC process is able to recover up to 92.4% of CO_2 with 96.6% H_2 purity. The energy requirement is of 0.19MJ_{el}/kg CO_2, this value is approximately over 2 times lower than that reported under comparable gas inlet conditions and separation specifications. It shows the possible potential of the concept for improved energy efficiency processes. However, this should be balanced regarding the total wide IGCC system energy requirement. H_2 loss is of 4.8% which is higher than that reported for conventional packed column based process (less than 1%). This result from the fact that no pressure flash is used with the HFMC process.

(ii) The overall mass transfer coefficient is of $1.2.10^{-5}$ m/s and $6.8.10^{-6}$ m/s in the absorber and desorber respectively. The $k_{ov,\,CO2}.a$ values obtained in this work are of 0.04 and 0.02 s^{-1} for the absorber and the desorber respectively.

(iii) Membrane mass transfer lower or at most comparable to that of absorbent mass transfer coefficient combined with higher CO_2/H_2 selectivity than that of the absorbent is required to increase the CO_2/H_2 process selectivity.

(iv) Lower H_2 loss is achieved at the expense of increased contactor size and liquid energy pumping energy.

A systematic and detailed parametric analysis (liquid and gas velocity, temperature, pressure, material permeation properties and module geometry) is needed in order to examine the interest of the HFMC loop process for a wide range of operating conditions. The potential of novel fiber geometry such as waves, helices or the addition of baffles to enhance the local mass transfer in the liquid phase could also be evaluated. These issues will be investigated in forthcoming papers.
The first simulation results of the proposed process raise several questions and the following perspectives can be proposed:

(i) In order to limit H_2 loss, a configuration using a flash at medium pressure to recover a portion of H_2 before entering the desorber contactor need to be investigated.

(ii) Isothermal 1D model is used to simulate the proposed process. Given the mass transfer limitation of the liquid phase, 2D model should be used in the simulation and compared to 1D simulation.

(iii) Experimental validation of the concept would be also of interest. The potential permeation of Selexol through the dense membrane skin should be evaluated in order to ensure stable absorption performances over long time scales.

APPENDICES

Appendix A

***Table A1**: Data of gas solubility and absorbent selectivity for CO_2/H_2 and CO_2/CH_4, at 25°C.*

	He'$_{CO2}$ =1/He$_{CO2}$ et 25°C $(C_L/C_G)_{eq}$	Selectivity CO_2/H_2	Selectivity CO_2/CH_4	Selectivity H_2S / CO_2
DMEPG	2.59 [f] 2.88 [e]	76.9[a] 63.8 [e] 76 [d]	14.92[a c e] 15.2[d]	8.93[a] 7.56 [e]
NMP	4.56[b]	156.25[a]	13.88 [a,b]	10.2[a]
PC	3.50[b]	128.2[a]	26.31 [a,b]	3.29_a
Water	0.82[b] 0.84 [c]		23.5 [a,b] 24.3 [c]	

[a] Bucklin and Schebdel, 1984, [b]*Dindore et al., 2004b* [c] *Sander,1999,* [d] *Kohl and Nielsen, 1997,* [e] Kapetaki *et al.,* 2015' [f] Rayer *et al*., 2011.

Table A2: Physico-chemical properties of some physical absorbents including Selexol, at 25°C.

	Viscosity (Pa.s) $\times10^3$ at 25°C	Vapor pressure(Pa) at 25°C	Freezing point (°C)	Molecular weight (g/mol)	Boiling point (°C)	Density at 25°C Kg/m^3	Surface tension mN/m
DMEPG	5.80 [a,f] 5.88 [h]	0.097 [f]	-28[a]	280[a]	240[b]	1030	33.5 [f] 32 [i]
Methanol	0.6 [b] 0.55 [d]	-	-92[b]	32.04	65 [b]	785	22.07 [d] 22.2 [e]
NMP	1.65[a] 1.68 [c] 1.69 [d] 1.7 [f]	52 [a] 53.33 [f]	-24[a]	99[a]	202[b,d]	1027	40.7 [d]
PC	3 [a] 2.5 [f]	11[a] 11.33 [f]	-48[a]	102[a]	240[b]	1195	41.5 [f]
Water	1[f]	3167.2 [f]	0[f]	18[f]	100[f]	1000	72.5 [d] 72.3 [f]

[a] Bucklin and Schebdel, 1984 , [b] *Kohl and Nielsen,1997,* [c] *Tian et al, 2012* , [d] *Wang 1996,* [e] *Yong, 1981,* [f] *Dindore, 2004b,* [g] Sander, 1999, [h]Heintz, 2011, [i] Siefert *et al*., 2016.

APPENDIX B

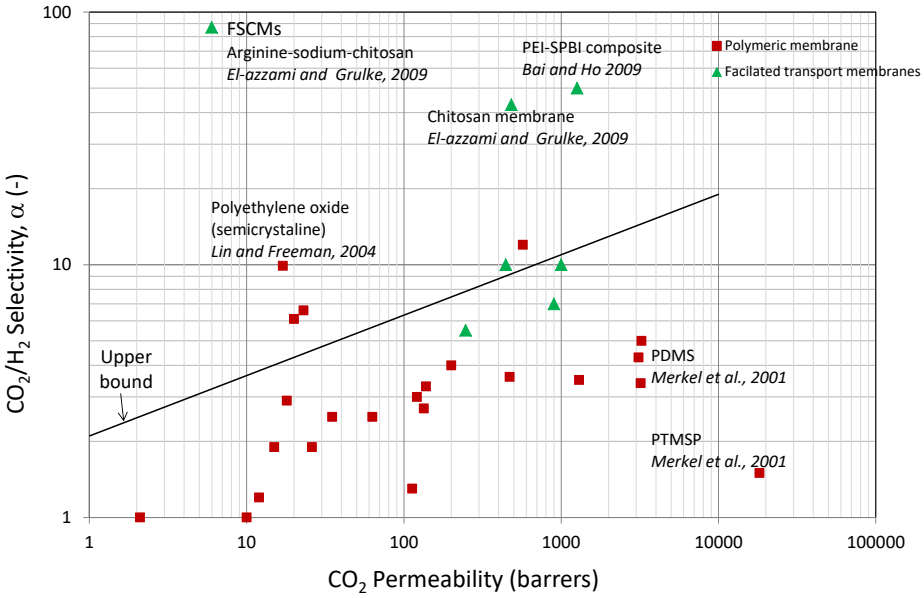

Figure B1: Data of polymeric membranes and advanced facilated transport membrane for CO_2/H_2 separation (Scholes *et al*., 2010, Elazzami and Grukle, 2009, Bai and Ho, 2009, Lin and Freeman, 2004, Merkel *et al*., 2001). Contrary to H_2/CO_2 upper bound, that for CO_2/H_2 separation shows a positive slope.

Table B2: Example of polymeric membrane for CO_2/H_2 separation [**1**].

Membrane	CO_2 permeability (barrer)	CO_2/H_2 selectivity (-)	$K_{M\ CO2}$ (for a 1μm thick membrane) m/s	T (°C)	P (bar)	Reference
Cross-linked Poly(ethylene glycol) acrylate (XLPEO)	570	12	$4.89.10^{-4}$	35	1	Lin and freeman, 2004
PDMS	3100	4.3	$2.6.10^{-3}$	35	5	Merkel et al., 2000
FSTM (arginine, sodium, Chitosan)	1500	144	$1.6.10^{-3}$	110	1.5	El-Azzami and Grukle, 2009
PEBAX	20	6.1	$1.65.10^{-5}$	25	4	Kim et al., 2001
PTFEP	470	3.6	$4.03.10^{-4}$	35	13.6	Nagai et al., 2000
PTMSP	18200	1.5	$1.56.10^{-2}$	35	1.4	Merkel et al., 2001

Appendix C

Resistances in series approach based on film theory is classically used for membrane contactors simulation purposes (**Gabelman and Hwang, 1999**). The local overall mass transfer coefficients can be expressed according to the resistance- in series model as follows:

The local absorbed CO_2 molar flux of specie *i* is expressed as:

$$N_{G,i}\left(mol.m^{-3}.s^{-1}\right)= a_m k_{ov,i}\left(C_{G,i} - C^*_{G,i}\right) \qquad \text{(C1)}$$

Where:

$$\frac{1}{k_{ov,i}} = \frac{He_i.d_{ml}}{d_e.k_{L,i}} + \frac{1}{k_{m,i}} + \frac{d_{ml}}{d_i.k_{G,i}} \qquad \text{(C2)}$$

$$C^*_{G,i} = He_i.C_{L,i} \qquad \text{(C3)}$$

a is the specific membrane module interfacial area (m^{-1}).

C_i^* is the hypothetical local gas-phase concentration in equilibrium with the liquid phase.

$k_{ov,i}$ is the local global mass transfer coefficient of specie $_i$. $k_{L,i}$, $k_{M,i}$, $k_{G,i}$ are the local effective membrane mass transfer coefficients of the liquid, the membrane and the gas phase respectively.

d_{int}, d_{ext} d_{ml} are the inner, outer and log mean diameters of the hollow fiber membrane. *He* is the Henry constant of the gas compound with water (defined as : $He= C_G\ (mol/m^3)/C_L\ (mol/m^3)$) .

In this model, the film theory (diffusion in boundary layer) is applied in the liquid and gas phases. The key assumptions of the 1D model are:

- Constant membrane mass transfer ($k_{m,i}$) coefficient
- Thermodynamic equilibrium at the gas–liquid interface

In laminar flow through a cylindrical pipe, gas and liquid mass transfer coefficient, k_G and k_L respectively can be estimated by integrating the Graetz equation (**Beek, 1999, Skelland, 1985, Levêque, 1928)** for suitable boundary conditions.

The Sherwood number in each phase is estimated by:

if $Gz < 0.03$ then $Sh=1.3Gz^{-1/3}$ (C4)

if $Gz > 0.03$ then $Sh=4.36$ (C5)

With Graetz and Sherwood numbers defined as follows (z is the axial coordinate):

$$Gz = \frac{D.z}{u_G.d_h^{\,2}} \qquad \text{(C6)}$$

$$Sh = \frac{kd_h}{D} \qquad \text{(C7)}$$

With d_h the hydraulic diameter.

For the gas phase, flowing in the lumen side, d_h corresponds to the internal fiber diameter (d_i).

The 1D model takes into account the evolution of the local mass transfer coefficients, the evolution of gas velocity (due to CO_2 absorption) and fluid pressure through the axial coordinate (z). Liquid velocity is supposed to be constant along the membrane length (i.e. negligible change in liquid molar flow due to gas absorption or desorption).

The differential equation system which is solved is detailed hereafter (n is the components number):

For the absorber:

- Gas differential molar balance:

$$\frac{dG_i}{dz} = -N_{G,i} \quad i = 1, n-1 \qquad \text{(C8)}$$

- Liquid differential molar balance:

$$\frac{dL_i}{dz} = -N_{G,i} \quad i = 1, n-1 \qquad \text{(C9)}$$

- Gas momentum balance (Hagen-Poiseuille) :

$$\frac{dP_G}{dz} = -\frac{32 u_G \mu_G}{d_{\text{int}}^{\ 2}} \qquad \text{(C10)}$$

$$u_G = \frac{RT}{P_G} \frac{1}{S_G} \sum_{i=1}^{n} G_i \qquad \text{(C11)}$$

With S_G, the gas flow section (m^2)

The boundary conditions are:

$$G_{G,i,z=0} = G_{z=0} \times y_{i,z=0}, \quad i = 1, n-1 \qquad \text{(C12)}$$

$$C_{L,i,z=Z} = C_{L,i,0} \quad i = 1, n-1 \qquad \text{(C13)}$$

$$C_{L,i,z=0} = C_{L,i,z=0}(initialisation) \quad i = 1, n-1 \qquad \text{(C14)}$$

For the desorber:

- Liquid differential molar balance:

$$\frac{dL_i}{dz} = -N_{G,i} \quad i = 1, n-1 \qquad \text{(C15)}$$

$$y_i = \frac{N_{G,i}}{\sum N_{G,i}} \quad i = 1, n-1 \qquad \text{(C16)}$$

The gas mass transfer resistance was supposed negligible.

The boundary conditions are:

$$C_{L,i,z=0} = C_{L,i,z=0}(initialisation) \quad i = 1, n-1 \qquad \text{(C17)}$$

$$C_{L,i,z=Z} = C_{L,i,0} \quad i = 1, n-1 \qquad \text{(C18)}$$

With

$$L_i = u_L C_{i,L} \qquad \text{(C19)}$$

$$G_i = u_G C_{i,G} \qquad \text{(C20)}$$

G_i, L_i, is the molar flow rate of compound *i* in the gas phase and in the liquid phase respectively.

For the liquid phase flowing in the shell side in laminar regime, Happel equation is used:

$$\Delta P_L = \frac{\kappa \mu_L}{d_{ext}} \frac{\varphi^2}{(1-\varphi)^2} u_L Z \qquad \text{(C21)}$$

κ is the Kozeny factor expressed by :

$$\kappa = 150\varphi^4 - 314.44\varphi^3 + 241.67\varphi^2 - 83.039\varphi + 15.97 \qquad \text{(C22)}$$

With ϕ the packing ratio and Z the contactor length.
Equations system is numerically solved with the appropriate boundary conditions through a Matlab computer code.

NOMENCLATURE

Latin symbols

a : Specific gas-liquid interfacial area (m^{-1})
d_h : Hydraulic diameter (m)
d_{int} : Internal fiber diameter (m)
d_{ext} : External fiber diameter (m)
d_{ml} : Log mean fiber diameter (m)
S_G : Gas flow section (m^2)
D_{int} : Internal membrane module diameter (m)
Z : Total contactor length (m)
Sh : Sherwood number (-)
Re : Reynolds number (-)
Sc : Schmidt number (-)
Gz : Graetz number (-)
C : Molar concentration ($mole.m^{-3}$)
C_G^* : Hypothetical local gas-phase concentration in equilibrium with the liquid phase ($mol.m^{-3}$)
D_i : Diffusion coefficient ($m^2 \cdot s^{-1}$)
Gz : Graetz number (-)
k : Mass transfer coefficient ($m \cdot s^{-1}$)
k_{ov} : overall mass transfer coefficient ($m.s^1$)
N_i : Molar flux ($mol\ m^{-2}\ s^{-1}$)
P : Pressure (Pa)
ΔP : Fluid pressure drop (bar)
ΔP_m : Transmembrane pressure difference (bar)
Q : Fluid volumetric flow rate ($m^3.s^{-1}$)
G : Gas molar flow rate ($mol.s^{-1}$)
L : Liquid molar flow rate ($mol.s^{-1}$)
T : Temperature (K)
y : Molar fraction in the gas (-)
u : Interstitial fluid velocity ($m \cdot s^{-1}$)
He : Henry constant (C_G/C_L) (-)
z : Axial coordinate (m)

G_{des} : Molar flow rate the stripped gas in the desorber
$P_{G,des}$: Vacuum pressure in the desorber (Pa)
$P_{L,p}$: Pumping power requirement for the reciulation of the abosrbent (W)
P_{vacuum} : Power required for vacuum pumping in the desorber for CO_2 stripping (W)

Greek symbols

φ : Module packing fraction (-)
μ : Viscosity ($Pa \cdot s^{-1}$)
ρ : Density ($kg \cdot m^{-3}$)
η_{CO2} : CO_2 removal efficiency (-)
Ω : Contactor cross section (m^2)
η_V : Vacuum pump efficiency (-)

Subscripts/ Exponents

i : Compound
G : Relative to gas
L : Relative to liquid
m : Relative to the membrane
in : Relative to fluid inlet
out : Relative to fluid outlet
abs : Relative to the absorber
des : Relative to the desorber

Abbreviations

HFMC : Hollow Fiber membrane contactor
PTMSP : Poly[1-(trimethylsylil)-1-propyne]
PTMGP : Poly[1-(trimethylgermil)-1-propyne]
PMP : Poly[4-methyl-2-pentyne]
PDMS : Polydemythyl siloxane
PTMSP : Poly[1-(trimethylsilyl)-1-propyne]
PTFE : Polytetrafluoroethylene
PP : Polypropylene
NMP : *N*-Methyl-2-pyrrolidone
PC : Propylene carbonate,
MEA : Monoethanolamine
DEA : Diethanolamine
MDEA : N-methyldiethanolamine
AMP : 2-amino-2-methyl-1-propanol
DEAE : 2-diethylaminoethanol
PZ : Piperazine
[Bmim][TCM] : 1-Butyl-3-methylimidazolium tricyanomethanide

References

Albarracin Zaidiza, D., Belaissaoui, B., Rode, S., Favre, E., 2017. Intensification Potential of Hollow fiber Membrane Contactors for CO_2 Chemical Absorption and Stripping using Monoethanolamine solutions, Separation and Purification Technology, 188, 38-51.

Albarracin Zaidiza, D., Wilson, S. G., Belaissaoui, B., Rode, S., Castel, C., Roizard, D., Favre, E., 2016. Rigorous modelling of adiabatic multicomponent CO_2 post-combustion capture using hollow fiber membrane contactors, Chemical Engineering Science, 145, 45-58.

Albarracin Zaidiza, D., Billaud, J., Belaissaoui, B., Rode, S., Roizard, D., Favre, E., 2014. Modeling of CO_2 post-combustion capture using membrane contactors, comparison between one- and two-dimensional approaches, Journal of Membrane Science, 455, 64-74.

Bai, H. and Ho, W. S. W., 2009. New Carbon Dioxide-Selective Membranes Based on Sulfonated Polybenzimidazole (SPBI) Copolymer Matrix for Fuel Cell Applications, Ind. Eng. Chem. Res. 48, 2344–2354.

Beek W.J., Muttzall K.M.K., Heuven J.W., 1999. Transport Phenomena, Wiley.

Bucklin, R. W. and Schendel, R. L., 1984. Comparison of Fluor Solvent and Selexol Processes: Physical solvent processes can be very useful for acid gas removal applications. Energy Progress, 4, 137-142

Casero, P., García Pena, F., Coca, P., Trujillo, J., 2014. ELCOGAS 14 MWth pre-combustion carbon dioxide capture pilot. Technical & economical achievements. Fuel 116, 804–811.

Chabanon, E., Belaissaoui, B.., Favre, E., 2014. Gas–liquid separation processes based on physical solvents: opportunities for membranes, Journal of Membrane Science, 459, 52-61.

Cui, Z. and deMontigny, D., 2013. "Part 7: A review of CO_2 capture using hollow fiber membrane contactors," Carbon Manag., 4 (1), 69–89.

Dai, Z., Ansaloni, L., and Deng L., 2016. Precombustion CO_2 Capture in Polymeric Hollow Fiber Membrane Contactors Using Ionic Liquids: Porous Membrane versus Nonporous Composite Membrane, DOI: 10.1021/acs.iecr.6b01247. Ind. Eng. Chem. Res., 55, 5983−5992.

Dave, A., Dave, M., Huang, Y., Rezvani, S., Hewitt, N., 2016. Process design for CO_2 absorption from syngas using physical solvent DMEPEG, International Journal of Greenhouse Gas Control 49, 436–448

Davidson, O., Metz, B., 2005. Special Report on Carbon Dioxide Capture and Storage, International panel on climate Change, Geneva, Switzerland /http:// www.ipcc.chS.

Drioli, E., Curcio, E., Di Profio G.,2005. State of the Art and Recent Progresses in Membrane Contactors, Chemical Engineering Research and Design, 83 (3) , 223-233.

Dindore, V.Y., Brilman, D.W.F., Geuzebroek, F.H., Versteeg, 2004a. G.F., Membrane–solvent selection for CO_2 removal using membrane gas–liquid contactors, Separation and Purification Technology, 40, 133–145.

Dindore, V.Y., Brilman, D.W.F., Feron, P.H.M., Versteeg, G.F., 2004b. CO_2 absoption at elevated pressures using a hollow fiber membrane contactor, J. Membr. Sci., 235, 99–109.

El-Azzami, L. A., Grulke, E. A., 2009. Carbon dioxide separation from hydrogen and nitrogen Facilitated transport in arginine salt–chitosan membranes, Journal of Membrane Science 328, 15–22

Falk-Pedersen, O., Dannstroem, H., Methods for Removing Carbon Dioxide from Gases, WO 98/04339 Kvaerner ASA, Norway.

Jansen, D., Gazzani, M., Manzolini, Van Dijk, G., E., Carbo, M., 2015. Pre-combustion CO_2 capture, International Journal of Greenhouse Gas Control 40, 167–187.

Gottlicher, G. and Pruschek, R., 1997. Comparaison of CO_2 removal systems for fossil-fuelled power plant process, Energy Convers. Mgmt, 38, S173-S178.

Gabelman, A., Hwang, S-T, 1999. Hollow fiber membrane contactors, Journal of Membrane Science, 159 (1-2, 61-106.

Heintz, Y. J., 2011. carbon dioxide capture from fuel gas streams under elevated pressures and temperatures using novel physical solvents, Doctor of Philosophy dissertation, November 29, the Swanson School of Engineering

Heile, S., Rosenberger, S., Parker, A., Jefferson, B., McAdam E.J., 2014. Establishing the suitability of symmetric ultrathin wall polydimethylsiloxane hollow-fibre membrane contactors for enhanced CO_2 separation during biogas upgrading, Journal of Membrane Science 452, 37-45

Kerber, J., Repke, J-U, 2016. Mass transfer and selectivity analysis of a dense membrane contactor for upgrading biogas, Journal of Membrane Science, 520, 450-464.

Kapetaki Z., Brandani, P., Brandani, S., Ahn, H.g, 2015. Process simulation of a dual-stage Selexol process for 95% carbon capture efficiency at an integrated gasification combined cycle power plant, International Journal of Greenhouse Gas Control 39, 17–26.

Kohl, A. L. and Nielsen, R. B., 1997. *Gas Purification*, 5th ed., Gulf Publishing Company, Houston, Texas.

Kwak, D-H., Yun, D., Binns, M., Yeo, Y-K. and Kim, J-K, 2014. Conceptual Process Design of CO_2 Recovery Plants for Enhanced Oil Recovery Applications, dx.doi.org/10.1021/ie502110q, Ind. Eng. Chem. Res. 53, 14385−14396.

Lévêque A., 1928. Les Lois de la transmission de chaleur par convection, Dunod, Paris, France.

Lin, H., Freeman, B.D., 2004. Gas solubility, diffusivity and permeability in poly(ethylene oxide), Journal of Membrane Science, 239 (1), 105-117.

Mohammed, I. Y., Samah, M., Mohamed, A., Sabina, G., 2014. Comparison of SelexolTM and Rectisol® Technologies in an Integrated Gasification Combined Cycle (IGCC) Plant for Clean Energy Production, International Journal of Engineering Research, 3 (12), 742-744.

Merkel, T.C, Gupta, R.P, Turk, B.S, Freeman, 2001. B.D, Mixed-gas permeation of syngas components in poly(dimethylsiloxane) and poly(1-trimethylsilyl-1-propyne) at elevated temperatures, Journal of Membrane Science, 191 (1–2), 85-94.

Merkel, T.C., Bondar, V.I., Nagai, K., et al., 2000. Gas sorption, diffusion, and permeation in poly(dimethylsiloxane), journal of polymer science part b-polymer physics, 38 (3), 3415-434.

Kim, J.H., Ha, S.Y., Lee, Y.M., 2001. Gas permeation of poly(amide-6-b-ethylene oxide) copolymer, Journal of membrane science, 190 (2), 179-193.

Nagai, K, Freeman, BD, Cannon, A, et al., 2000. Gas permeability of poly(bis-trifluoroethoxyphosphazene) and blends with adamantane amino/trifluoroethoxy (50/50) polyphosphazene , Journal of membrane science, 172 (1-2), 167-176.

Nguyen, P.T., Lasseuguette, Medina-Gonzalez, E., Y., Remigy, J.C., Roizard, D., Favre, E., 2011. A dense membrane contactor for intensified CO_2 gas/liquid absorption in post-combustion capture, Journal of Membrane Science, 377, 261-272.

Ozturk, B. and Hughes, R., 2012. Evaluation of mass transfer characteristics of non-porous and microporous membrane contactors for the removal of CO_2, Chemical Engineering Journal, 195–196, 122-131

Padurean, A., Cormos, C.-C., Agachi, 2012. P.S., Pre-combustion carbon dioxide capture by gas–liquid absorption for Integrated Gasification Combined Cycle power plants, International Journal of Greenhouse Gas Control 7, 1–11.

Park, S., Lee, S., Wook Lee, J., Chun, S. N., Lee, J. B., 2015. The quantitative evaluation of two-stage pre-combustion CO_2 capture processes using the physical solvents with various design parameters, Energy 81, 47-55.

Rayer, A.V., Henni, A. and Tontiwachwuthikul, P., 2012. High Pressure Physical Solubility of Carbon Dioxide (CO2) in Mixed Polyethylene Glycol Dimethyl Ethers (Genosorb 1753), the canadian journal of chemical engineering, 90, 576-583

Scholes,C. A., Smith, K.H., Kentish, S. E., Stevens G. W., 2010. CO_2 capture from pre-combustion processes—Strategies for membrane gas separation, International Journal of Greenhouse Gas Control 4, 739–755.

Scholes A. C., Simioni, M., Qader, A., Stevens, G. W., Kentish, S. E., 2012. Membrane gas–solvent contactor trials of CO_2 absorption from syngas, Chemical Engineering Journal 195–196, 188–197.

Siefert, N.S., Agarwal, S., Shi, F., Shi, W., Roth, E.A., Hopkinson, D., Kusuma, V.A., Thompson, R.L., Luebke, D.R., Nulwala, H.B., 2016. Hydrophobic physical solvents for pre-combustion CO_2 capture: Experiments, computational simulations, and techno-economic analysis, International Journal of Greenhouse Gas Control 49, 364–371.

Skelland A.H. P., 1985. Diffusional Mass Transfer, R.E. Krieger Pub. Co.

Sander R.,1999. Compilation of Henry's Law Constants for Inorganic and Organic Species of Potential Importance in Environmental Chemistry. http://www.mpch-mainz.mpg.de/~sander/res/henry.html

Theo, W. L., Lim, J. S., Hashim, H., Mustaffa A. A., Ho W. S., 2016. Review of pre-combustion capture and ionic liquid in carbon capture and storage, Applied Energy 183, 1633–1663.

Trusov, A., Legkov, S., Van den Broeke, L. J.P., Goetheer, E., Volkov, A., 2011. Gas/liquid membrane contactors based on disubstituted polyacetylene for CO_2 absorption liquid regeneration at high pressure and temperature. Journal of Membrane Science, 383 (1-2), 241-249.

Tian, S., Hou, Wu, Y. W., Ren, S. and Pang K., 2012. Physical Properties of 1-Butyl-3-methylimidazolium Tetrafluoroborate/N-Methyl-2-pyrrolidone Mixtures and the Solubility of CO_2 in the System at Elevated Pressures, American Chemical Society 756 dx.doi.org/10.1021/je200886j, J. Chem. Eng. Data, 57(2012) 756−763.

Wang, D., Li, K., Teo, W.K., 1996. Polyethersulfone hollow fiber gas separation membranes prepared from NMP/alcohol solvent systems, Journal of Membrane Science 115, 85-108.

Yong S. Won, Dong K. Chung, and Mills, A. F., 1981. Density, Viscosity, Surface Tension, and Carbon Dioxide Solubility and diffusivity of Methanol, Ethanol, Aqueous Propanol, and Aqueous Ethylene Glycol at 25 °C, J. Chem. Eng. Data, 26, 141-144.